

# Rheological Properties of Solutions of a Polyampholytic Block Copolymer

Tomomitsu Sekitani<sup>1</sup>, Kenji Urayama<sup>1</sup>, Manabu Tsuruta<sup>2</sup>, Masahiko Mitsuzuka<sup>2</sup>, and Toshikazu Takigawa<sup>1</sup>

**Abstract** Steady shear flow behavior as well as dynamic viscoelasticity was investigated for solutions of a polyampholytic block copolymer. Benzyl alcohol solutions of the polymer show behavior common to usual polymer solutions, whereas the aqueous solutions form transient networks at short times. Shear thickening and shear thinning emerge on the flow curves of the aqueous solutions at high shear rates. Curves of dynamic loss modulus ( $G''$ ) for the aqueous solutions move to the long time side by the application of steady shear. The increase in relaxation intensity also occurs by shear. The shift of the  $G''$  curves to the long time side disappears but a long time is required for the recovery. The origin of the shear thickening is related not only to the shift of the curves but also to the increase in relaxation intensity. These changes on the  $G''$  curves are originated from a developed microphase separation under shear flow.

**Keywords** Associative polymer • Shear thickening • Shift of relaxation time • Increased relaxation intensity • Shear-induced development of microphase separation

## Introduction

Polymer solutions forming transient networks show unique rheological properties. Specifically, most of the systems undergo shear thickening at high shear rates [1–7]. The transient network systems might be divided into two categories. One is the systems composed of polymer chains and

small-sized crosslinkers, and the other is so-called associative polymer systems. Aqueous solutions of poly(vinyl alcohol) (PVA) and sodium borate [1–3] belong to the former, and hydrophobic ethoxylated urethanes (HEURs) are typical of the latter [4–7], both of which show shear thickening. Until now much work, in experimental [1–7] and theoretical [8–11] approaches, has been made to clarify the origin of the shear thickening in a microscopic level. The results provide several possibilities for the shear thickening (for example, non-Gaussian elasticity of polymer chains [9–11]), but they are still in controversy. The origin of the shear thickening in the microscopic level may be different if the category differs, but causes in phenomenological rheology must be common for both categories.

The aim of this study is to examine the origin of the shear thickening of an associative polymer system belonging to the latter category: more directly, to survey experimental evidences for long time relaxations causing the shear thickening under flow.

## Experimental

The polymer sample used in this study is a commercial polymer sample-coded as VSR-50K (Mitsui Chemicals Polyurethanes Inc., Japan). Figure 1 shows the chemical structure of VSR-50K: the polymer is polyampholytic, composed of poly(ethylene glycol) (PEG), hexyldiisocyanate and comb-shaped diol units, the ratio  $n/m$  being 6. Number and weight average molecular weights ( $M_n$  and  $M_w$ , respectively), reduced to the molecular weight of the equivalent size of PEG, are reported to be  $M_n = 1.5 \times 10^5$  and  $M_w = 4.1 \times 10^5$ . The powdery sample was dissolved in pure water at 80°C to obtain aqueous solutions. The concentration for aqueous solutions was fixed to be 1 %. Benzyl alcohol solutions at various concentrations were also prepared in the similar way. According to the supplier's data sheet, benzyl alcohol is one of good solvents for the polymer VSR-50K. In calculating the polymer

T. Takigawa (✉)

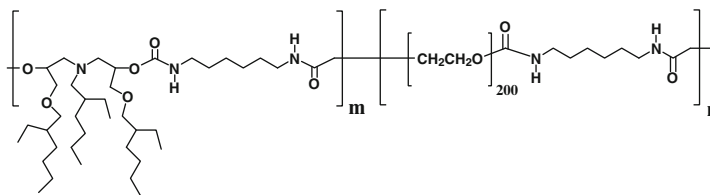
<sup>1</sup>Department of Material Chemistry  
Kyoto University

Nishikyo-ku, Kyoto 615-8510, Japan  
e-mail: takigawa@rheogate.polym.kyoto-u.ac.jp

<sup>2</sup>R&D Center

Mitsui Chemicals Polyurethanes Inc.,  
Sodegaura, Chiba 299-0265, Japan

**Fig. 1** Chemical structure of VSR-50K



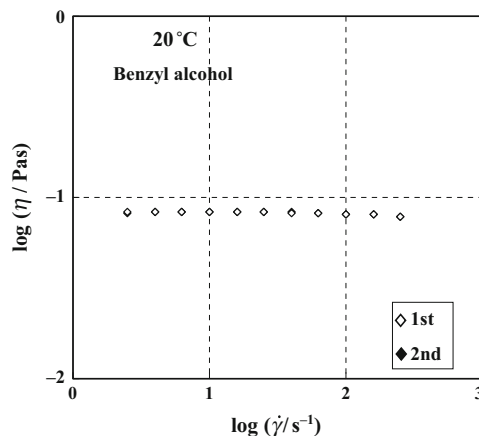
concentration ( $c$ ) in  $\text{kg m}^{-3}$ , the density  $1.046 \text{ g cm}^{-3}$  was employed for benzyl alcohol and the density  $1.0 \text{ g cm}^{-3}$  was assumed for VSR-50K.

Rheological measurements were performed with a strain-controlled type rheometer (ARES; Rheometric Scientific, USA) or a stress-controlled type (DAR-100; Reologica, Sweden) at 10 and 20°C. ARES was chiefly used to examine the effect of the strain amplitude on dynamic viscoelastic functions of the aqueous solutions with a cone-plate geometry (diameter, 50 mm; cone angle, 0.04 rad). The strain amplitude ranged from 0.1 to 0.5. The rheometer DAR-100 was used for steady shear and dynamic viscoelasticity measurements. A bob-cup geometry was used for these measurements. The diameters of the bob and the cup were 25.0 mm and 26.7 mm, respectively. In angular frequency ( $\omega$ ) and shear rate ( $\dot{\gamma}$ ) sweeps the scans were made in the low-to-high direction.

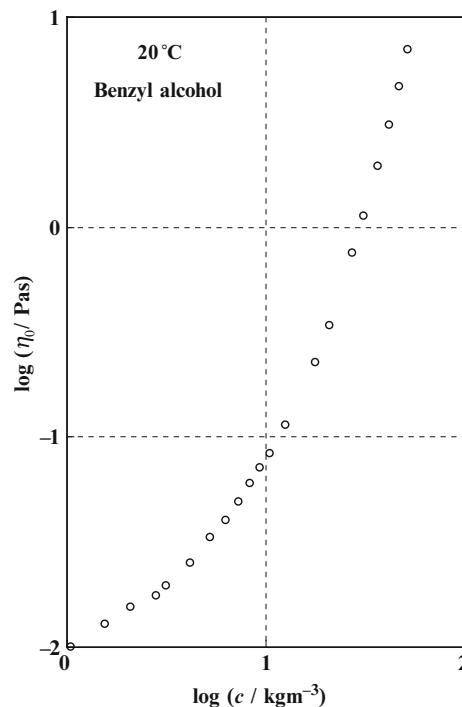
## Results and discussion

Figure 2 shows steady shear viscosity ( $\eta$ ) plotted against  $\dot{\gamma}$  for the 1 % solution of VSR-50K in benzyl alcohol at 20°C. Here, the 2nd run measurement was made immediately after the 1st run was completed. The two curves are well coincided and are almost independent of  $\dot{\gamma}$  over the range of  $\dot{\gamma}$  examined. Similar behavior was observed for solutions at other concentrations. The leveling-off value of  $\eta$  corresponds to the zero-shear viscosity ( $\eta_0$ ) of the solution. Figure 3 shows the  $c$  dependence of  $\eta_0$  for VSR-50K in benzyl alcohol at 20°C. The  $c$  dependence becomes strong with increasing  $c$ . By applying a two-line approximation to the dependence curve, a concentration at the intersection ( $c_c$ ; a critical concentration dividing the dilute and the semi-dilute regimes by the viscosity profile) can be estimated to be ca.  $15 \text{ kg m}^{-3}$  (ca. 1.5 %).

In Fig. 4  $\omega$  dependence curves of the dynamic storage and loss moduli ( $G'$  and  $G''$ , respectively) of the 1% aqueous solution, measured with an ARES rheometer at 20°C, are shown. The applied strain amplitude here was 0.3, but almost the same curves were obtained for the other strain amplitudes up to 0.5. A tail of plateau on the  $G'$  curve and a broad peak on the  $G''$  curve are observed in the high  $\omega$  region. Typical flow behavior is observed in the intermediate



**Fig. 2** Plot of viscosity ( $\eta$ ) plotted against shear rate ( $\dot{\gamma}$ ) for VSR-50K in benzyl alcohol at 20°C



**Fig. 3** Concentration ( $c$ ) dependence of the zero-shear viscosity ( $\eta_0$ ) for VSR-50K in benzyl alcohol at 20°C

and low  $\omega$  region: the slope of the  $G''$  curve is identical to unity, but that of the  $G'$  curve is slightly smaller than 2. These suggest that a network structure is formed in the

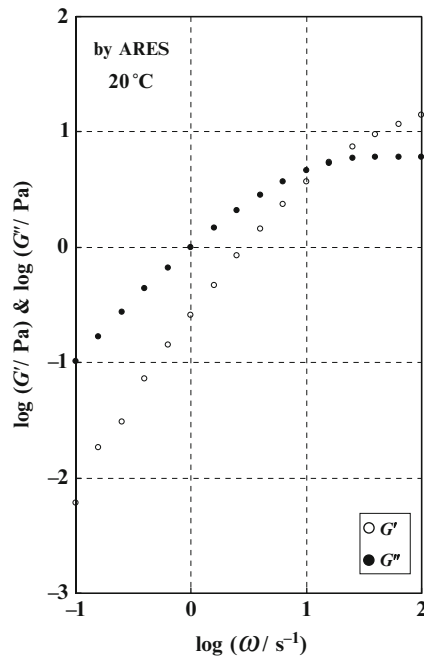


**Fig. 4** Dynamic storage modulus ( $G'$ ) and loss modulus ( $G''$ ) plotted against angular frequency ( $\omega$ ) for 1 % aqueous solution of VSR-50K at 20°C

aqueous solution at short times. Because the polymer sample VSR-50K is a multi-block copolymer composed of hydrophobic and hydrophilic blocks, a microphase-separated structure works as a network: hydrophobic domains, i.e., aggregates of hydrophobic blocks, act as physical crosslinks and hydrophilic blocks interconnect the crosslinks. Since the fact that the slope of the  $G'$  versus  $\omega$  curve is smaller than 2 means that the relaxation times have a distribution, we define an average relaxation time ( $\tau_p$ ) for the dynamic viscoelasticity as a reciprocal of  $\omega$  where the  $G'$  and  $G''$  curves intersect. This relaxation time corresponds to pulling-out of hydrophobic block chains from the crosslink domains. At 20°C,  $\tau_p$  is estimated to be 0.06 s.

Figure 5 shows  $\dot{\gamma}$  dependence curves of  $\eta$  obtained from  $\dot{\gamma}$  sweep tests for the 1 % aqueous solution at 20°C. For both of the 1st and 2nd runs,  $\eta$  in the low  $\dot{\gamma}$  region is almost independent of  $\dot{\gamma}$ , giving  $\eta_0$  of the solution. However, the values are different: the value for the 2nd run is higher than that for the 1st run. It should be noted here that even  $\eta_0$  for the 1st run is about 10 times higher than that for the benzyl alcohol solution because of the formation of the transient network. In the intermediate region of  $\dot{\gamma}$ , shear-thickening is observed on the both curves, and the 2nd run is still located in the upper side compared with the 1st run. In the high  $\dot{\gamma}$  region, shear thinning occurs with increasing  $\dot{\gamma}$ , but the 1st and 2nd runs coincide well with each other. Figure 6 shows double-logarithmic plots of shear stress ( $\sigma$ ) versus  $\dot{\gamma}$  obtained from the  $\dot{\gamma}$  sweep tests shown in Fig. 5. In the low  $\dot{\gamma}$  region, the 2nd run is shifted upwards compared with the 1st run, but both are

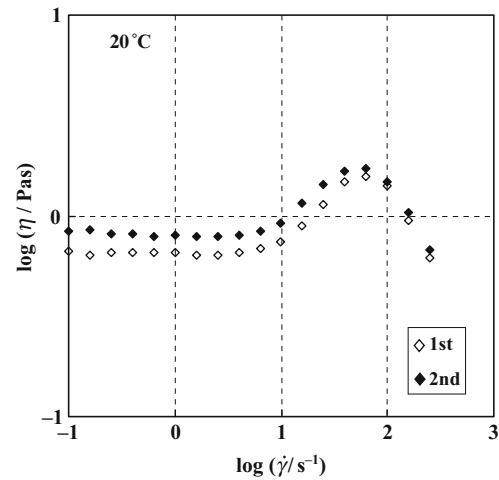


**Fig. 5** Viscosity ( $\eta$ ) plotted against shear rate ( $\dot{\gamma}$ ) for 1 % aqueous solution of VSR-50K at 20°C

linear with a slope of unity. In the intermediate region of  $\dot{\gamma}$ , shear-thickening emerges as a steep rise on each curve. As is the case of Fig. 5, the both curves coincide with each other at high  $\dot{\gamma}$ , where a plateau (“yielding” region) is clearly observed. The  $G''(\omega)$  curves before and after steady shear measurements with a DAR-100 rheometer are also included in this figure. In the low  $\dot{\gamma}$  ( $\omega$ ) region, the  $G''$  curve before shear traces out the 1st run of  $\sigma$ ; an empirical relation that the  $G''$ – $\omega$  curve becomes identical to the  $\sigma$ – $\dot{\gamma}$  curve if  $\omega$  is equated with  $\dot{\gamma}$  holds for the VSR-50K solution. The  $G''$  curve after shear is shifted upwards compared with that before shear and is close to the 2nd run of  $\sigma$  in position. Comparing the peak position of the two  $G''$  curves a very small shift to the long time side as well as an increase in  $G''$  due to the application of shear flow is observed. To clarify the peak shift on the  $G''$  curves by high shear flow,  $\omega$  sweep tests were conducted again for  $G''$  at 10°C. A lower temperature (10°C) was chosen because the  $G''$  curve was expected to move to the low  $\omega$  side by lowering temperature. The results are shown in Fig. 7: the curve after steady shear flow (at  $\dot{\gamma} = 2.5 \times 10^2 \text{ s}^{-1}$  for 600 s) exhibits a peak shift to the long time side as well as an increase in  $G''$  value. The peak shift corresponds to the increase of  $\tau_p$ . About 16 h after shear, the  $G''$  curve recovers the original position before shear.

It was confirmed that the application of flow did change neither shape nor position of the 2nd runs (for  $\eta$  and  $\sigma$ ) or the  $\omega$  dispersion curve of  $G''$  after shear, as long as the value of  $\dot{\gamma}$  did not exceed  $10 \text{ s}^{-1}$ , which corresponds to the position of  $\dot{\gamma}$  ( $\omega$ ) where the dynamic and steady flow data branch out (Fig. 6), at 20°C. This means that if we monitor a  $G''$  value after the 2nd run no reduction in  $G''$  value occurs for this region of  $\dot{\gamma}$ . We observed that the reduction of  $G''$  really occurred for  $\dot{\gamma}$  larger than  $10 \text{ s}^{-1}$ . The degree of reduction in  $G''$  and a characteristic time for the reduction ( $\tau_s$ ; a recovery

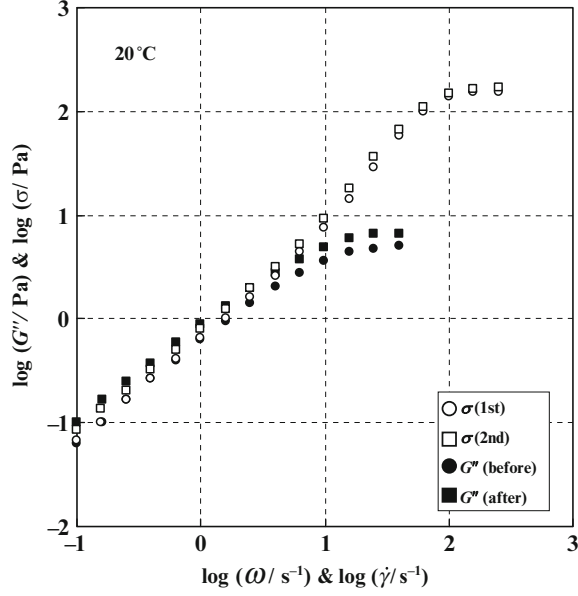


**Fig. 6** Shear stress ( $\sigma$ ) plotted against shear rate ( $\dot{\gamma}$ ) for 1 % aqueous solutions of VSR-50K at 20°C. The  $\omega$  dependence of dynamic loss modulus ( $G''$ ) is also plotted

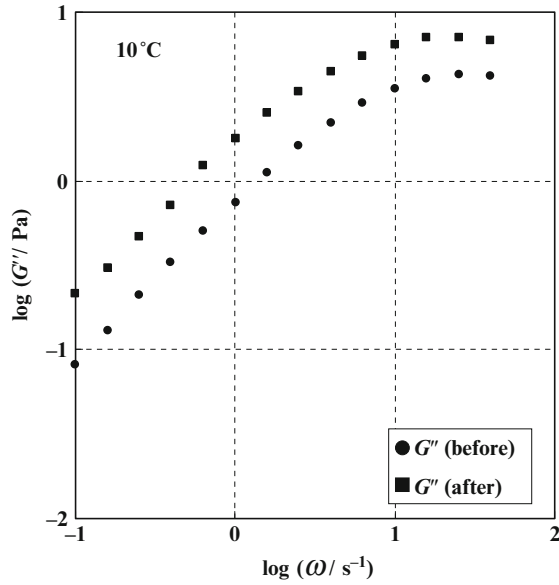


**Fig. 7** Loss modulus ( $G''$ ) plotted against angular frequency ( $\omega$ ) before and after shear at 10°C

time to the original structure) was rather short when  $\dot{\gamma}$  lay in the region of  $10 \text{ s}^{-1} < \dot{\gamma} < 70 \text{ s}^{-1}$ : for example,  $\tau_s$  at  $\dot{\gamma} = 20 \text{ s}^{-1}$  for  $600 \text{ s}^{-1}$  was estimated to be the order of magnitude of 10 s. For  $\dot{\gamma} > 70 \text{ s}^{-1}$ , the degree of reduction increased and  $\tau_s$  also became very long. An example is shown in Fig. 8. Figure 8(a) shows a  $t$  dependence curve of  $G''$  measured at  $\omega = 1 \text{ s}^{-1}$  after the cessation of the shear flow as an example. The value

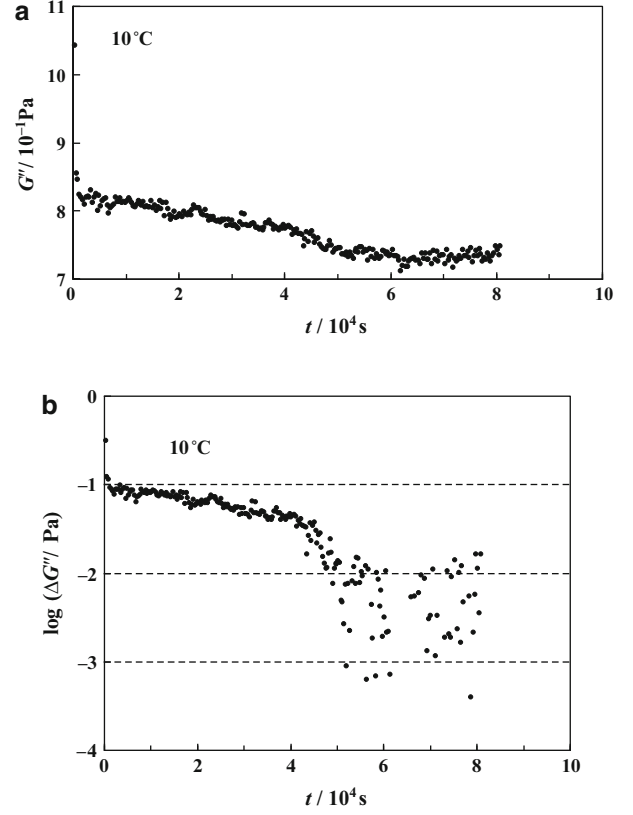


**Fig. 8** (a) Time ( $t$ ) dependence of  $G''$  at  $\omega = 1 \text{ s}^{-1}$  after shear; (b) Semi-logarithmic plot of  $\Delta G''$  against time ( $t$ ). For the definition of  $\Delta G''$ , see text

of  $\dot{\gamma}$  applied here is beyond the value at which the  $\eta_0$  curve shows a peak. After a steep decrease of  $G''$  at very short times the value gradually decreases with increasing  $t$  but levels off at long times. To evaluate  $\tau_s$ , we define  $\Delta G''(t)$  by  $\Delta G''(t) = G''(t) - G''_\infty$  with  $G''_\infty$  being an average of  $G''$  in the leveling-off region. Then, we assume the functional form  $\Delta G''(t) = A \exp(-t / \tau_s)$  at long times, where  $A$  is a constant. In Figure 8(b) a semi-logarithmic plot of  $\Delta G''(t)$  versus  $t$  is shown. The data points over a fairly wide range of  $t$  can be approximated by a single line, giving  $\tau_s$  of ca.  $5 \times 10^4 \text{ s}$ . Beyond the  $\dot{\gamma}$  value where the peak emerges on the  $\eta_0$  curves, the shear thinning was observed. This thinning occurs because very high shear flow causes a large scale change in structure such as a breakdown of the microphase-separated structure. In this case, a very long time (large value of  $\tau_s$ ) is required for recovery.

At 20°C, the shear thickening occurred in the region of  $10 \text{ s}^{-1} < \dot{\gamma} < 70 \text{ s}^{-1}$ . Why the shear-thickening occurs by the application of high shear flow can be understood in terms of the linear viscoelasticity theory. Since the  $G''$  curve becomes a crude approximation to the relaxation spectrum  $H$  if we set  $\omega = 1 / \tau$  [15], we have

$$H(\tau) \cong \frac{2}{\pi} [G''(\omega)]_{\omega=1/\tau} \quad (1)$$

Defining a relaxation spectrum under shear flow at  $\dot{\gamma}$   $H(\tau, \dot{\gamma})$  by

$$H(\tau, \dot{\gamma}) \cong \frac{2}{\pi} [G''(\omega, \dot{\gamma})]_{\omega=1/\tau} \quad (2)$$

the steady shear viscosity at  $\dot{\gamma}$  can be calculated by

$$\begin{aligned} \eta(\dot{\gamma}) &= \int_{-\infty}^{\infty} \tau H(\tau, \dot{\gamma}) d \ln \tau \\ &\cong \frac{2}{\pi} \int_{-\infty}^{\infty} \tau G''(\omega, \dot{\gamma})_{\omega=1/\tau} d \ln \tau \end{aligned} \quad (3)$$

Here,  $G''(\omega, \dot{\gamma})$  stands for the loss modulus under the flow at  $\dot{\gamma}$ , and thus this is a virtual quantity. Equation (3) states that the shift and increase of  $G''$  in the flow field enhance the viscosity, giving an explanation for the shear thickening for the aqueous solutions. The increased value of  $\eta_0$  at the 2nd run results from the similar origin; the enhancement is due to the aftereffect of flows at the 1st run and is thus only transient.

The origin of the shift and increase of  $G''$  under flow is not clear at present. One possible reason for the changes is the development of the microphase separation by flow. The aqueous solutions of VSR-50K show the shear thickening at low temperatures (10 and 20°C), but at an elevated temperature (60°C), no shear thickening was observed for the aqueous solutions. This suggests that the VSR-50/water system has a phase diagram with an upper critical solution temperature (UCST). In addition, the system is highly viscoelastic due to the existence of the microphase separated structure, i. e., transient network structure. This kind of system has a possibility of a marked shear-induced phase separation if the system stays just above the coexistence curve [12, 13]. If the system is located in the two-phase region, the application of shear increases a quench depth; namely, the shear flow develops the microphase separation. An increase in the

number of crosslink domains and also an increase in the dimension as well as rigidity of the domains must originate from the development of the microphase separation by shear flow. The degree of development is expected to increase with increasing  $\dot{\gamma}$ . The developed structure can move back to the original one after the cessation of shear flow. The recovery proceeds rather fast (small value of  $\tau_s$ ) when the applied  $\dot{\gamma}$  is not so high ( $\dot{\gamma} < 70 \text{ s}^{-1}$  at 20°C), because the recovery is attained only by partial dissolution. At high  $\dot{\gamma}$ , however, the recovery process is composed of the partial dissolution and the large scale change in microphase separated structure. Thus, this recovery process becomes very slow because the latter takes long time.

**Acknowledgements** This work was partly supported by a Grant-in-Aid for Scientific Research on Priority Area “Soft Matter Physics” (No. 19031014) from the Ministry of Education, Culture, Sports, Science and Technology of Japan.

## References

1. Savins JG (1968) *Rheol Acta* 7: 87
2. Maerker JM, Sinton SW (1986) *J Rheol* 30: 77
3. Inoue T, Osaki K (1993) *Rheol Acta* 32: 550
4. Annable T, Buscall R, Ettelaie R, Whittlestone D (1993) *J Rheol* 37: 695
5. Yekta A, Xu B, Duhamel J, Adiwidjaja H, Winnik MA (1995) *Macromolecules* 29: 2229
6. Tam KC, Jenkins RD, Winnik MA, Bassett DR (1998) *Macromolecules* 31: 4149
7. Berert J-F, Serero Y, Whinkelman B, Calvet D, Collet A, Viguier M (2001) *J Rheol* 45: 477
8. Witten TA, Cohen MH (1985) *Macromolecules* 18: 1915
9. Vrahopoulou EP, McHugh AJ (1987) *J Rheol* 31: 371
10. Marrucci G, Bhargava S, Cooper SL (1993) *Macromolecules* 26: 6483
11. Indei T, Koga T, Tanaka F (2005) *Macromol Rapid Commun* 26: 701
12. Hashimoto T, Fujioka K (1991) *J Phys Soc Jpn* 60: 356
13. Imaeda T, Furukawa A, Onuki A (2004) *Phys Rev E* 70: 051503

Gels: Structures, Properties, and Functions

Fundamentals and Applications

Tokita, M.; Nishinari, K. (Eds.)

2009, IX, 213 p. 210 illus., 11 illus. in color., Hardcover

ISBN: 978-3-642-00864-1